Estimation of screening length and electric charge on particles in single-layered dusty plasma crystals

Chieko Totsuji,[1,*] M. Sanusi Liman,[2] Kenji Tsuruta,[1] and Hiroo Totsuji[1]
[1]*Department of Electrical and Electronic Engineering, Faculty of Engineering, Okayama University, Tsushimanaka 3-1-1, Okayama 700-8530, Japan*
[2]*Graduate School of Natural Science and Technology, Okayama University, Tsushimanaka 3-1-1, Okayama 700-8530, Japan*
(Received 26 March 2003; published 3 July 2003)

Single-layered two-dimensional crystals of dust particles are often observed in dusty plasma experiments and the data on their structure can be obtained by analyzing the images usually taken by charge-cupled device cameras. We give here some formulas for practical purposes of estimating the screening length and the electric charge on a dust particle from the surface density and the radius of such finite two-dimensional dust crystals. The formulas are derived on the basis of our theoretical approach which has been successful in reproducing results of molecular-dynamics simulations on dusty plasmas. An example of application is also shown.

DOI: 10.1103/PhysRevE.68.017401 PACS number(s): 52.27.Lw, 52.27.Jt, 52.65.Yy

Dusty plasmas have been attracting our attention since the first observation of their ordered structures. In dusty plasmas we are able to clearly observe structures and dynamic properties of strongly coupled plasmas. We have investigated the structure formation and melting of dusty plasmas in two- and three-dimensional, finite and infinite systems by molecular-dynamics simulations and theoretical analyses. We have reproduced vertically layered structures observed in experiments [1] by molecular dynamic simulations, modeling the system as a collection of charged particles which interact with each other via the screened Coulomb (Yukawa) interaction and are vertically confined by a balance between the gravity and the electric field due to electrode [2,3]. The number of layers changes discretely with two system parameters, the strengths of confinement and screening. We have also developed a theory with intralayer cohesive (correlation) energy and succeeded in reproducing results of our simulations [2,3]. We have also performed numerical simulations and theoretical analyses on the mixture of dust particles with different charge-to-mass ratios and found the separation of species by gravity [4].

The dusty plasma system takes the single-layered (two-dimensional) structure in the limit of strong confinement [2]. These single-layer dust crystals have been used to observe static and dynamic properties of strongly coupled plasmas [5]. When the system is finite, as in the case of real experiments, such a single-layered dusty plasma can be modeled as Yukawa particles that interact with each other via the Yukawa potential

$$q^2\exp(-r/\lambda)/r, \tag{1}$$

where q is the electric charge on a dust particle and λ the screening length, and are in the horizontal two-dimensional parabolic potential

$$\tfrac{1}{2}kR^2, \tag{2}$$

where $R^2=x^2+y^2$ is the radial distance from the center of the potential. At low temperatures, this system is characterized by only two parameters

$$\alpha=q^2/(k\lambda^3) \tag{3}$$

and the number of particles, N [7]. Simulations have been performed for the system containing up to 10^4 particles, and structures in equilibrium states are obtained. For large system, we have applied the fast multipole method to compute mutual interactions [6,7].

In this Brief Report, we discuss the estimation of screening length λ and electric charge q from the information obtained in experiments and derive some formulas for practical purposes. As an example, we apply the results to experiments [8,9].

We have proposed a theoretical approach based on the variational method and have shown that our theoretical analysis reproduces the results of simulation almost completely for large systems when parameter α exceeds 1 [7]. The most important element of our theory is the inclusion of the cohesive (correlation) energy between dust particles. The details are given in Ref. [7]. The theory gives the surface density of particles, ρ, as a function of distance from center, R, in a dimensionless form,

$$\lambda^2\rho\left(\frac{R}{\lambda}\right)=\frac{1}{4\pi\alpha}\left[\left(\frac{R_m}{\lambda}\right)^2-\left(\frac{R}{\lambda}\right)^2\right]+\frac{3a}{4\pi}\left\{\frac{1}{4\pi\alpha}\left[\left(\frac{R_m}{\lambda}\right)^2-\left(\frac{R}{\lambda}\right)^2\right]+\left(\frac{a}{8\pi}\right)^2\right\}^{1/2}+\frac{5a^2}{32\pi^2} \tag{4}$$

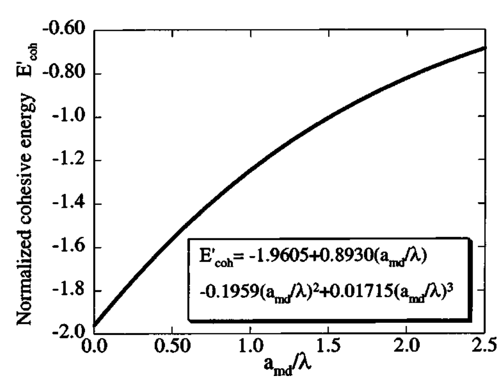

FIG. 1. Cohesive energy of the two-dimensional triangular Yukawa lattice.

*Email address: totsujic@elec.okayama-u.ac.jp

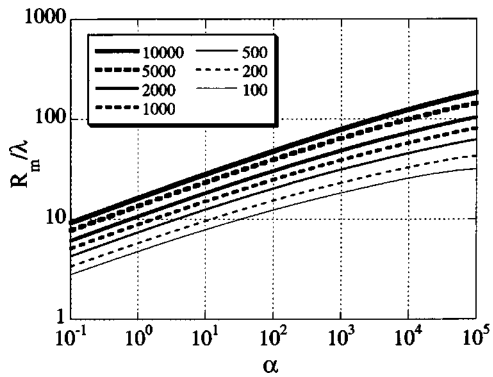

FIG. 2. Relation between R_m/λ and parameter α for various values of the number of particles N.

for $R<R_m$ and

$$\lambda^2\rho\left(\frac{R}{\lambda}\right)=0 \tag{5}$$

for $R>R_m$. Here R is the distance from the center of the system and R_m is the maximum radius of the system, determined by

$$8\alpha N=\left(\frac{R_m}{\lambda}\right)^4+\frac{2a}{\sqrt{\pi}}\alpha^{1/2}\left\{\left[\left(\frac{R_m}{\lambda}\right)^2+\frac{a^2}{16\pi}\alpha\right]^{3/2}-\left(\frac{a^2}{16\pi}\alpha\right)^{3/2}\right\}+\frac{5a^2}{4\pi}\alpha\left(\frac{R_m}{\lambda}\right)^2. \tag{6}$$

Parameter a in the above expressions is determined numerically from cohesive energy of the triangular Yukawa lattice in two dimensions, E_{coh} [3], as follows. When the surface density is n, the mean distance of particles is given by $a_{md}=(\pi n)^{-1/2}$. The normalized cohesive energy $E'_{\mathrm{coh}}=E_{\mathrm{coh}}/(q^2/a_{md})$ is a function of ratio $\ell=a_{md}/\lambda$ and is interpolated by a polynomial as shown in Fig. 1. In a limited range of ℓ, the cohesive energy can be approximated as a linear function of ℓ. We use linear approximation around $\ell=\ell_1$, where $\ell_1=(R_m/\sqrt{N})/\lambda$ is the average mean distance of particles in the two-dimensional circular crystal of N particles with radius R_m normalized by λ. Parameter a is defined so that $-a\sqrt{\pi}$ is the linearly extrapolated (normalized) energy for $\ell=0$, when one linearly approximates $E'_{\mathrm{coh}}(\ell)$ around ℓ_1:

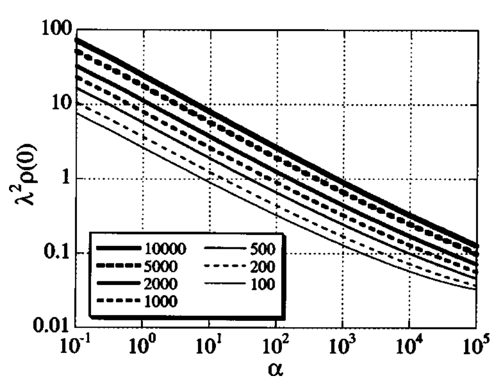

FIG. 3. Relation between $\lambda^2\rho(0)$ and parameter α for various values of the number of particles N.

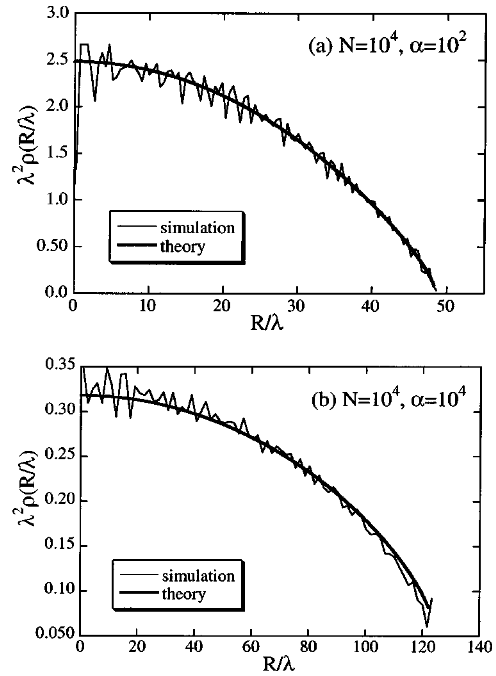

FIG. 4. Examples of radial distributions of number density obtained by simulation and theory, including 10^4 particles. The distance from the center of the distribution is normalized by screening length λ and (a) $\alpha=10^2$ and (b) $\alpha=10^4$.

$$-a\sqrt{\pi}=E'_{\mathrm{coh},0}=E'_{\mathrm{coh}}(\ell)\bigg|_{\ell=\ell_1}-\ell\frac{dE'_{\mathrm{coh}}(\ell)}{d\ell}\bigg|_{\ell=\ell_1}$$
$$=-1.9605+0.195\,94\,\ell_1^2-0.034\,298\,\ell_1^3. \tag{7}$$

Relations (4)–(6) are derived within the above approximation of linear dependence of $E'_{\mathrm{coh}}(\ell)$ on ℓ. We first solve Eqs. (6) and (7) self-consistently to obtain a: Since ℓ_1 and a depend on R_m/λ and vice versa, small number of iterations are necessary. The density distribution is then given by Eqs. (4) and (5).

The values of R_m/λ and $\lambda^2\rho(R=0)$ are shown in Figs. 2 and 3, respectively, as functions of α for various values of

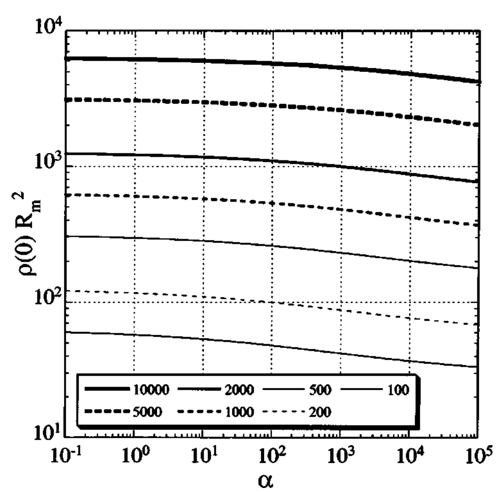

FIG. 5. Relation between $\rho(0)R_m^2$ and parameter α with various values of the number of particles N.

number of particles, N. Typical examples of the distribution of particles obtained by simulations and reproduced by theory are shown in Fig. 4.

Single-layered dusty plasma crystals are often observed in experiments in parallel-plate discharge chambers. The data on their structures can be obtained by analyzing the images taken by charge-couupled device cameras. Let us now consider extracting information on physical quantities related to dust particles from these experiments on the basis of our theory.

In Fig. 5, the dimensionless values $\rho(0)R_m^2$ in our theory are shown as functions of α for various values of number of particles, N. In experiments, on the other hand, the number of particles, N, the maximum radius R_m, and the central density $\rho(0)$ may be easily determined for each crystal. We can thus estimate the value of α from the experimental values of N and $\rho(0)R_m^2$, inverting the relation between $\rho(0)R_m^2$ and α. Once α is estimated, we can obtain λ and q if the value of k is known: λ and q are evaluated from $\rho(0)$ (or R_m) and k. As is shown below, the information on k is given independently in some cases. Even if the value of k is not exactly known, the identification of α is useful in evaluating plasma conditions.

For practical purposes, we give here approximate but directly applicable expressions for α in terms of N and $\rho(0)R_m^2$:

$$\log_{10}\alpha = f_1+f_4\ln\frac{f_2-[\rho(0)R_m^2-f_3]}{f_2+(\rho(0)R_m^2-f_3)}, \tag{8}$$

where for $10^2\leqslant N\leqslant 10^3$,

$$f_1=1.0605N^{0.1703},$$

$$f_2=-0.1694N-7.208\times 10^{-6}N^2,$$

$$f_3=0.4607N-4.447\times 10^{-6}N^2,$$

$$f_4=-1.4138+1.2304N^{-0.9307}-5.981\times 10^{-5}N;$$

and for $10^3\leqslant N\leqslant 10^4$,

$$f_1=1.3024N^{0.1399},$$

$$f_2=-0.1866N-9.838\times 10^{-7}N^2,$$

$$f_3=0.4522N-1.4606\times 10^{-6}N^2,$$

$$f_4=-1.9280+1.0543N^{-0.1208}.$$

TABLE I. Examples of experimental data [8].

N	s_0 (mm)	R_m (mm)	ρ_0 (mm^{-2})	$\rho_{\rm ave}$ (mm^{-2})
1161	0.41	10.31	6.80	3.48
434	0.52	6.88	4.35	2.92
276	0.58	5.88	3.41	2.54
205	0.61	5.35	3.08	2.28
106	0.71	4.18	2.28	1.93

When $10<\alpha<10^5$, the relative error of the above expression is less than 9% and when $1<\alpha<10$, less than 10% for $10^2<N<9\times 10^2$ and less than 17% for $9\times 10^2<N<10^4$. Since the values of the screening length and charge are not so sensitive to α, their values can be estimated to the first two digits based on the above expression.

We also give approximate expressions for $R_{\rm m}/\lambda$ in terms of N and α:

$$\log_{10}\left(\frac{R_{\rm max}}{\lambda}\right)=g_1+g_2\log_{10}\alpha+g_3(\log_{10}\alpha)^2, \tag{9}$$

where for $10^2\leqslant N\leqslant 10^4$,

$$g_1=0.1204+0.2906\log_{10}N-4.199\times 10^{-3}(\log_{10}N)^2;$$

for $10^2\leqslant N\leqslant 10^3$,

$$g_2=0.2324-9.613\times 10^{-3}\log_{10}N+3.991\times 10^{-3}(\log_{10}N)^2,$$

$$g_3=-3.045\times 10^{-2}+1.300\times 10^{-2}\log_{10}N-2.010\times 10^{-3}(\log_{10}N)^2;$$

and for $10^3\leqslant N\leqslant 10^4$,

$$g_2=0.1735+3.263\times 10^{-2}\log_{10}N-3.545\times 10^{-3}(\log_{10}N)^2,$$

$$g_3=-9.913\times 10^{-3}-1.489\times 10^{-3}\log_{10}N+5.307\times 10^{-4}(\log_{10}N)^2.$$

The relative error of the above expression is less than 1%.

As an example, we apply our formulas to experiments by Hebner *et al.* [8,9]. Some of their experimental data are listed in Table I. The values of nearest neighbor separation at the center of distribution s_0 and maximum radius R_m are taken from Figs. 5 and 6 in Ref. [8] for each case with different number of particles, N. The density at center $\rho(R$

TABLE II. Estimation of screening length and electric charge.

N	$\rho(0)R_m^2$ (Experiment)	Estimated α	$\rho_0\lambda^2$ (Theory)	R_m/λ (Theory)	λ (mm)	$q(e)$
1161	723.7	0.061 ± 0.001	33.70 ± 0.02	4.63 ± 0.05	[a]	[a]
434	206.3	$(5.09\pm 0.23)\times 10^2$	0.300 ± 0.001	26.2 ± 0.1	0.26	1.9×10^4
276	118.0	$(1.99\pm 0.14)\times 10^3$	0.145 ± 0.001	28.6 ± 0.1	0.21	2.5×10^4
205	88.3	$(1.29\pm 0.01)\times 10^3$	0.152 ± 0.001	24.1 ± 0.1	0.22	2.3×10^4
106	39.7	$(7.99\pm 0.20)\times 10^3$	0.063 ± 0.001	25.0 ± 0.1	0.17	3.7×10^4

[a]Our theory is not applicable to the case where $\alpha<1$.

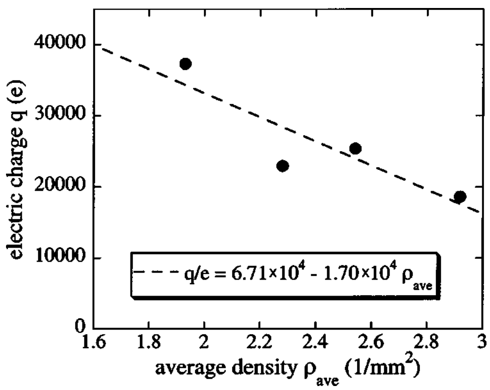

FIG. 6. Estimated electric charge as the function of the average number density ρ_{ave}.

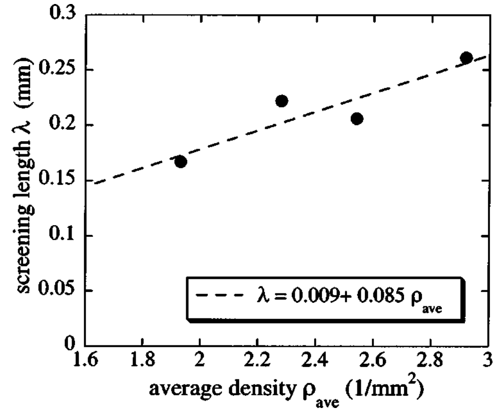

FIG. 7. Estimated screening length as the function of the average number density ρ_{ave}.

$=0$) is calculated from s_0 by $\rho(0)=2/(\sqrt{3}s_0^2)$ since the particles are ordered into the regular triangular lattice in the central region. The average number density of the particles, ρ_{ave} may be estimated by $\rho_{\mathrm{ave}}=N/(\pi R_m^2)$.

After determining α, we estimate λ and q from the experimental values of $\rho(0)$ (or R_m) and k: In these experiments, the confining parameter is given by $k=m_d g/R_c$ and is equal to 8.6×10^{-12} kg/sec^2, where $m_d=4.4\times10^{-13}$ kg is mass of a melamine particle of where diameter is 8.34 μm, g is gravity acceleration, and $R_c=0.5$ m is curvature of the electrode.

The results are shown in Table II. In the case of $N=1161$, the estimated value of α is 0.029 and is beyond the applicability of our theory. The obtained values of electric charge and screening length are shown in Figs. 6 and 7 as a function of average density. Our estimation of the screening length is consistent with the estimation in Refs. [8,9] on the average and that of the charge on a particle is smaller. We also see that the screening length slightly increases and the charge almost linearly decreases with the increase in the number density of particles. Large scatter of points in Figs. 6 and 7 may be attributed to fluctuations in plasma conditions from experiment to experiment with different number of particles. In addition, the crystals are not exact circles in experiments and the values of R_m may also include ambiguity.

Our theoretical approach takes into account, as cohesive (correlation) energy, the interactions between not only neighboring but also distant particles. Since the screening lengths are of the same order of magnitude as the interparticle separation s_0 in these experiments, the interaction beyond the nearest neighbors cannot be neglected. Our result may indicate that smaller charge on each particle is enough to describe mutual interactions when interactions beyond nearest neighbors are taken into account.

Though the number of data points is small and one has to be careful in assuming the similarity of plasma conditions, our results suggest the possibility of more detailed analysis on the plasma parameters. In this case, the electric charge on individual particle and the screening length seem to have the decreasing and increasing tendencies, respectively, when we put larger number of particles into a finite plasma. The physical mechanism for these tendencies may, however, not be simple and is beyond the scope of this Brief Report. (The increase of λ with N and ρ_{ave} may suggest a decrease in the number density of electrons. The average charge density of particles, $q\rho_{\mathrm{ave}}$, however, seems also to slowly decrease with N and ρ_{ave}, implying an increase in the electron number density.) The experimental determinations of these parameters are still among the most important issues in dusty plasma physics and our formulas will be useful for those purposes.

This work was partly supported by the Grant-in-Aid for Scientific Research (B) from the Ministry of Education, Culture, Sports, Science and Technology of Japan, No. 08458109 and No. 11480110.

[1] For example, H. Thomas, G.E. Morfill, V. Demmel, J. Goree, B. Feuerbacher, and D. Mohlmann, Phys. Rev. Lett. **73**, 652 (1994); J.H. Chu and Lin I, Physica A **205**, 183 (1994); Phys. Rev. Lett. **72**, 4009 (1994).

[2] H. Totsuji, T. Kishimoto, and C. Totsuji, Phys. Rev. Lett. **78**, 3113 (1997).

[3] H. Totsuji, T. Kishimoto, and C. Totsuji, Jpn. J. Appl. Phys., Part 1 **36**, 4980 (1997).

[4] H. Totsuji, T. Kishimoto, C. Totsuji, and T. Sasabe, Phys. Rev. E **58**, 7831 (1998).

[5] For example, D.S. Samsonov, J. Goree, Z.W. Ma, A. Bhattacharjee, H.M. Thomas, and G. Morfill, Phys. Rev. Lett. **83**, 3649 (1999); D.S. Samsonov, A.V. Ivlev, R.A. Quinn, G. Morfill, and S. Zhdanov, *ibid.* **88**, 095004 (2002).

[6] H. Totsuji, Phys. Plasmas **8**, 1856 (2001).

[7] H. Totsuji, C. Totsuji, and K. Tsuruta, Phys. Rev. E **64**, 066402 (2001).

[8] G.A. Hebner, M.E. Riley, D.S. Johnson, P. Ho, and R.J. Buss, Phys. Rev. Lett. **23**, 235001 (2001).

[9] G.A. Hebner, M.E. Riley, and K.E. Greenberg, Phys. Rev. E **66**, 046407 (2002).